Journal of Molecular Catalysis A: Chemical 315 (2010) 76–81

Contents lists available at ScienceDirect

Journal of Molecular Catalysis A: Chemical

journal homepage: www.elsevier.com/locate/molcata

Theoretical study of TBD-catalyzed carboxylation of propylene glycol with CO_2

Jun Ma[a,b], Xuelan Zhang[a,b], Ning Zhao[a], Abdullah S.N. Al-Arifi[c], Taieb Aouak[c], Zeid Abdullah Al-Othman[c], Fukui Xiao[a], Wei Wei[a,*], Yuhan Sun[a,*]

[a] State Key Laboratory of Coal Conversion, Institute of Coal Chemistry, Chinese Academy of Sciences, Taiyuan 030001, PR China
[b] Graduate University of the Chinese Academy of Sciences, Beijing 100039, PR China
[c] Chemistry Department, King Saud University, Riyadh 11451, Saudi Arabia

ARTICLE INFO

Article history:
Received 14 July 2009
Received in revised form 2 September 2009
Accepted 4 September 2009
Available online 15 September 2009

Keywords:
Catalytic mechanism
TBD
DFT
CO_2
Propylene glycol

ABSTRACT

The mechanisms for the reaction of propylene glycol (PG) with CO_2 catalyzed by 1,5,7-triazabicyclo [4.4.0]dec-5-ene (TBD) were theoretically investigated by density functional theory (DFT) method at the B3LYP/6-311++G(d,p) level. Through analyzing the optimized structures and energy profiles along the reaction paths, the PG-activated route was identified as the most probable reaction path, in which the rate-determining step was the nucleophilic attack of one of the O atoms in CO_2 on the hydroxyl linked C atom in PG with energy barrier 56.96 kcal/mol. The catalytic role of TBD could be considered as a proton bridge activated by the synergistic action of its N atoms.

1. Introduction

Recently, the synthesis of propylene carbonate (PC) from propylene glycol (PG) and CO_2 has drawn much interest. Both homogeneous [1–5] and heterogeneous [6–8] catalysts have been reported to be effective in this carbonylation. In our previous work [4], an experimental study of the carbonylation of PG with CO_2 was carried out with organic bases as the catalysts. And 1,5,7-triazabicyclo[4.4.0]dec-5-ene (TBD) showed a superior catalytic activity compared to the others.

TBD is one of the non-ionic nitrogen bases which are widely used to catalyze the carbonylation of amines or alcohols with CO_2 as the carbonylation reagent [9–13]. Unfortunately, it was not clear how TBD weakened the barriers for the carbonylation. One possibility was the substrate activation, which made it more susceptible to the electrophilic attack of the CO_2 [10–15]. The other was the CO_2 activation, which makes it more active to attack [16–18]. However, only few studies on the description of reaction mechanisms or the possible structures of the carbonylation transition state were reported [14,15].

In the present work, the mechanisms for TBD-catalyzed carbonylation of PG with CO_2 were first proposed and then verified by quantum chemistry computations of DFT method.

2. Mechanism proposals

According to the two possibilities mentioned above, two mechanisms were proposed. They are presented here with the name PG-activated and CO_2-activated, respectively.

The catalytic activities of the organic bases are, in many cases, associated with their proton transfer activities [19], which would make the active site of the deprotonated molecule more susceptible to the electrophilic attack of the CO_2 [10]. TBD is a widely used proton transfer agent in acid–base catalyzations [20–24], especially the reactions involving proton transfer between hydroxyl compounds [25,26]. The consequence of the proton transfer from the hydroxyl to the TBD is a hydrogen bonded ion-pair. Half of which, the TBD protonated molecule ($TBDH^+$), has already been studied experimentally as well as theoretically [26–31].

Based on these considerations, a PG-activated mechanism for the TBD-catalyzed carbonylation reaction of PG with CO_2 was proposed in Scheme 1, which consisted of two consecutive steps. First, PG was activated via being looted one hydroxyl H by the N atom of TBD, accompanied by the electrophilic attack of CO_2 on the hydroxyl O atom giving rise to an "ion-pair" (**2** or **5**). This was the CO_2 electrophilic attack step. Next, with the proton migrating from $TBDH^+$ to the other hydroxyl group, a water formed and the oxygen of the bonded CO_2 nucleophilicly attacked the C atom of PG to afford PC, and the catalyst TBD was recovered. This was named as the dehydration step.

In the CO_2 electrophilic attack step, the proton shift and the O–C bond formation occurred simultaneously. This process is similar to

* Corresponding authors.
E-mail addresses: weiwei@sxicc.ac.cn (W. Wei), yhsun@sxicc.ac.cn (Y. Sun).

1381-1169/$ – see front matter © 2009 Elsevier B.V. All rights reserved.
doi:10.1016/j.molcata.2009.09.003

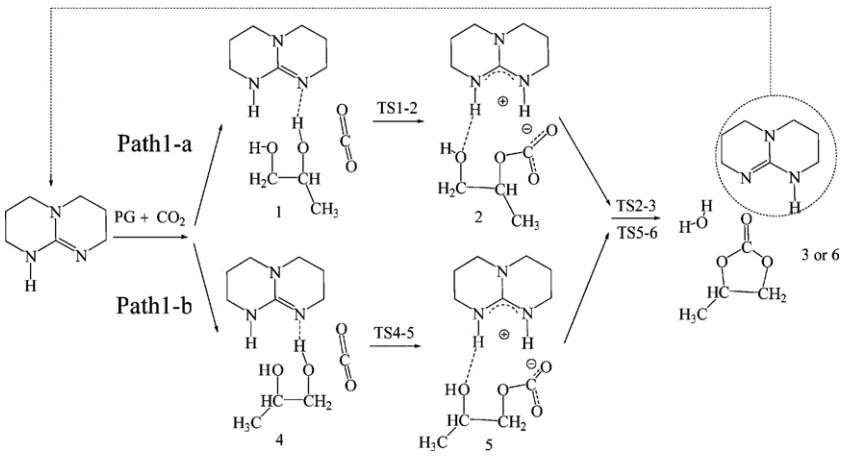

Scheme 1. PG-activated mechanism for carbonylation of PG with CO_2 via TBD.

the acid–base catalytic mechanism of Simn and Goodman [32], in which the transfer of H in methanol and the O–C bond formation occurred simultaneously and only one transition state was present. A similar reaction process, in which the proton shift and the O–C bond formation occurred simultaneously had also been reported by Aresta et al. [14] for the synthesis of dimethyl carbonate (DMC) from methanol and CO_2 with dicyclohexylcarbodiimide (CyN=C=NCy, DCC) as the catalyst.

In the dehydration step, the transfer of the proton hydrogen from $TBDH^+$ to the hydroxyl of PG yielded a water molecular. The leaving of the hydroxyl increased the positive charge of the C atom, making it unstable and tending to bond with other suitable atoms. This greatly facilitated the nucleophilic attack of the O atom in CO_2 on the C atom at the hydroxyl-lost site of PG. So it could be assumed that these occurred in one step and to be verified by the subsequent calculations.

According to the possible selection of reaction sites between the two hydroxyls of PG, two alternative paths were considered, corresponding to the dehydration of the primary hydroxyl (Path1-a) and the dehydration of the secondary hydroxyl (Path1-b), respectively.

For the CO_2-activated mechanism, the formation of an intermediate base–CO_2 adduct is the key step [19,33–35], which makes it more active to attack the substrate [16–18]. The base–CO_2 complexes are also efficient, clean and selective transcarboxylating reagents [16]. Especially, the TBD–CO_2, one of these complexes, shows an interesting thermal stability and has a well-defined structure verified both experimentally and theoretically [18,34].

To clarify the essential character of TBD–CO_2, the structures and population analysis of TBD, TBD–CO_2 and CO_2 were computed by DFT method at the B3LYP/6-311++G(d,p) level (see Fig. 1). Obviously, the original linear molecule CO_2 possessed a bond angle of 134.6° after bound to TBD. Its two C–O bonds were elongated from 1.161 Å to 1.240 Å and 1.214 Å, respectively. Comparing the charge distributions of the isolated CO_2 and the TBD–CO_2, it was found the total negative electric charge of CO_2 was enhanced from 0 e to −0.467 e. The charge of C atom almost unchanged, but the negative charges of O atoms were enhanced. These indicated that the charge was transferred from TBD to CO_2 and enriched at the O atoms, particularly the one close to the amino H. This suggested that the O atoms rather than the C atom in CO_2 were activated, due to the enhanced electronegativity.

Following the above considerations, the CO_2-activated mechanism was proposed in Scheme 2. It also consisted of a dehydration step and a CO_2 electrophilic attack step, besides the preliminary step of the TBD–CO_2 complex formation. As PG moved close to TBD–CO_2, one of its hydroxyl and the amino H atom of TBD combined to yield a H_2O. Subsequently, the hydroxyl-losing C in PG was nucleophilicly attacked by the activated O atom in TBD–CO_2. In the second step, TBD captured the H of the other hydroxyl in PG by its N atom, and then the electrophilic attack of the C atom in CO_2 on the hydroxyl O atom took place. Consequently, PC was

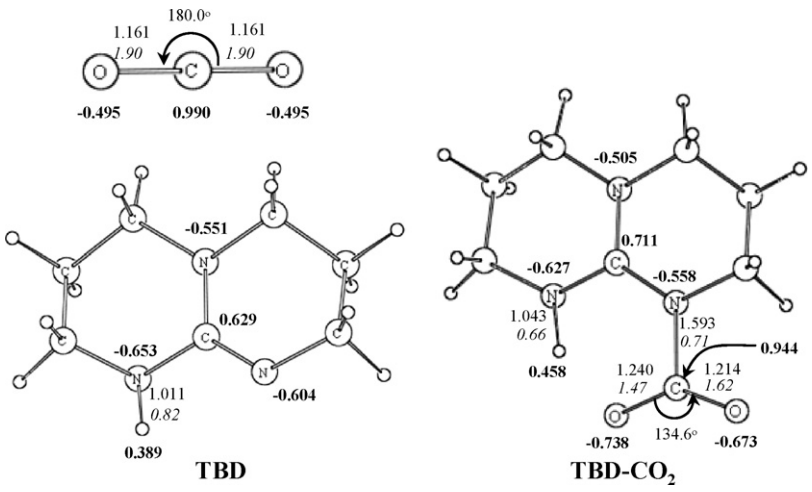

Fig. 1. Optimized geometries and charge distributions of TBD, CO_2 and TBD–CO_2 at the B3LYP/6-311++G(d,p) level. The bond distances (in angstroms), bond orders (italic), angles (in degrees) and atomic charges (bold) are labeled in the corresponding positions.

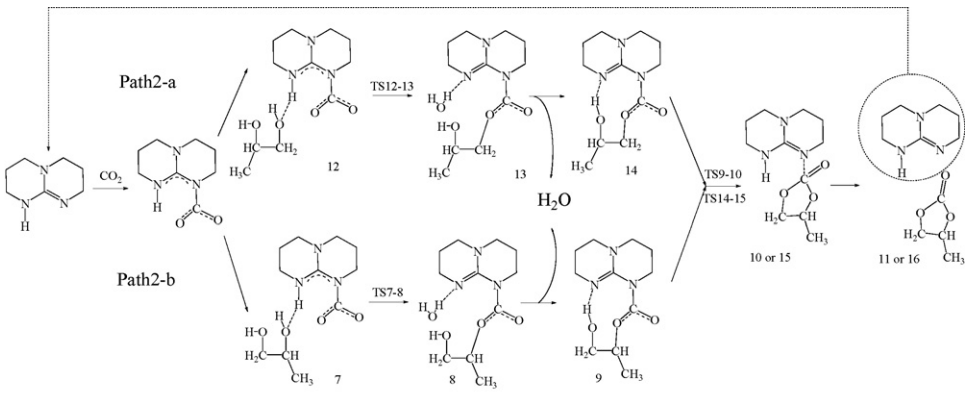

Scheme 2. CO_2-activated mechanism for carbonylation of PG with CO_2 via TBD.

formed and TBD recovered. It should be noted that the sequence of the CO_2 electrophilic attack step and the dehydration step was reversed compared to that of PG-activated mechanism.

In a word, two catalytic mechanisms, each consisted of two alternative reaction paths, were proposed for the TBD-catalyzed carboxylation of PG with CO_2. With the aim to verify the proposed mechanisms, these paths were computationally modeled through DFT method.

3. Computational methods

All calculations were carried out with the Gaussian03 package [36] using DFT method with Becke's three-parameter hybrid exchange functional and the Lee-Yang-Parr correlation functional (B3LYP) [37]. Initially, geometry optimizations and frequency calculations were made with 6-31+G(d) basis set [38–40], and then intrinsic reaction coordinate (IRC) calculations were performed to confirm a given transition state connecting a particular couple of consecutive minima on the proposed reaction pathways. To obtain more accurate results, all the geometries were re-optimized using the extended 6-311++G(d,p) basis set [38–40] followed by frequency calculations. The calculated energies were corrected by zero-point vibrational energies (ZPVE) with the scale factor 0.9804 [41]. Natural population analysis (NPA) and bond order analysis were performed using the NBO program in Gaussian03. Basis set superposition errors (BSSE) inherent in the computation of molecular interactions were also corrected via counterpoise technique [42,43].

Table 1
Zero-point vibration energies, total energies (electronic energy + ZPE) and relative energies of the reactants, intermediates, transition states, and final products of the carbonylation reaction of PG with CO_2 to synthesize PC, calculated at the B3LYP/6-311++G(d,p) level.

Species	Zero-point energy (hartree)	Total energy (hartree)	Relative energy (kcal/mol)
1	0.326076	−896.953256	0.00
TS1-2	0.323234	−896.941641	7.29
2	0.330233	−896.944837	5.28
TS2-3	0.324477	−896.843062	69.15
3	0.326590	−896.940837	7.79
4	0.326276	−896.951556	0.00
TS4-5	0.323444	−896.939781	7.39
5	0.330080	−896.943284	5.19
TS5-6	0.322375	−896.852520	62.15
6	0.326809	−896.941239	6.47
7	0.328056	−896.947442	0.00
TS7-8	0.322648	−896.847664	62.61
8	0.327449	−896.934186	8.32
9	0.303096	−820.480572	0.00
TS9-10	0.300388	−820.446407	21.44
10	0.302870	−820.449839	19.29
11	0.302374	−820.488751	−5.13
12	0.328495	−896.946037	0.00
TS12-13	0.321976	−896.842757	64.81
13	0.326519	−896.927825	11.43
14	0.303107	−820.483239	0.00
TS14-15	0.300957	−820.446269	23.20
15	0.302849	−820.449473	21.19
16	0.302334	−820.488249	−3.14

4. Results and discussion

Fig. S1 and Fig. S2 (in the Supplementary material) shows the predicted geometric structures of the intermediates and transition states along the reaction paths. Energies at the B3LYP/6-311++G(d,p) level are listed in Table 1. The BSSE-corrections calculated at the B3LYP/6-311++G(d,p) level are listed in Table 2. The total energy (electronic energy + ZPE) curves of PG-activated mechanism and CO_2-activated mechanism are presented in Figs. 2 and 3, respectively. The BSSE-corrections were found insignificant at the 6-311++G(d,p) basis set as shown in Table 2, Figs. 2 and 3. If not explicitly announced, energies in the following discussions are referred to those at the B3LYP/6-311++G(d,p) level without BSSE-corrections.

4.1. PG-activated mechanism

As proposed above, this mechanism involved two alternative channels, one corresponded to the dehydration of the primary hydroxyl group of PG (Path1-a), the other the dehydration of the secondary hydroxyl (Path1-b). Calculations confirmed that each path could take place in two consecutive steps, the CO_2 electrophilic attack step and the dehydration step, as depicted in Scheme 1.

As shown in Fig. S1, the precursor state of Path1-b was structure **4**, in which the primary hydroxyl group of PG had a weak electrostatic interaction with the C atom in CO_2 and an intermolecular hydrogen bond H1–N1 with TBD. The presence of hydrogen bond

Table 2
Calculated BSSE-correction (kcal/mol) at the B3LYP/6-311++G(d,p) levels.

Species	BSSE-correction	Species	BSSE-correction
1	1.47	7	0.68
2	1.45	8	1.46
3	1.67	11	0.65
4	1.54	12	0.83
5	1.53	13	1.03
6	1.69	16	0.72

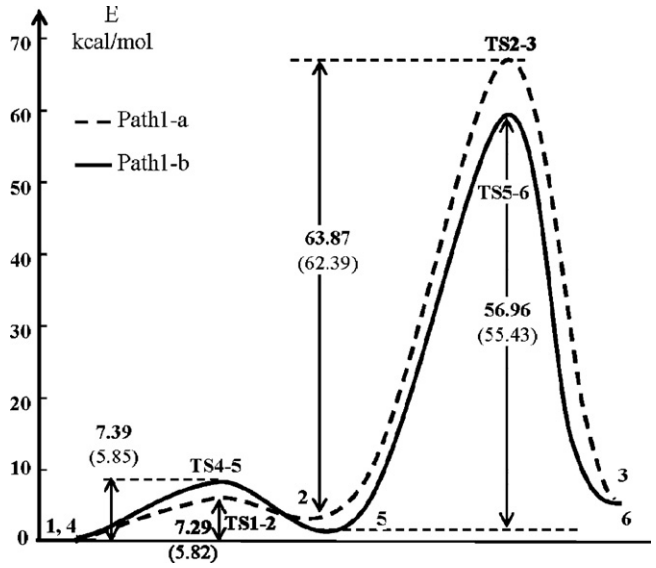

Fig. 2. The total energy (electronic energy + ZPE) curves of PG-activated mechanism of synthesis of PC from PG and CO_2 over TBD, calculated at the B3LYP/6-311++G(d,p) level. Energies including BSSE-corrections are also indicated in the parentheses.

suggested that proton transfer at this position should be straightforward. The transition structure TS4-5 (433.9*i* cm^{-1}) was formed as H1 swung from O1 to N1. It was noted that an accompanied process, i.e., the O1–C4 bond shrinking (from 2.759 Å to 2.053 Å) simultaneously occurred with bond order increased from 0.01 to 0.21. These indicated that electrophilic attack of CO_2 on the O1 atom of the primary hydroxyl of PG took place as the proton transferred from the same hydroxyl to the N1 atom of TBD. This led to the intermediate **5**, a hydrogen bonded ion-pair, one of which was the TBD protonated molecule ($TBDH^+$), the other was the anion $(CH_3)CH(OH)CH_2OC(O)O^-$ with charge −0.893 e. The migration of proton promoted the nucleophilic nature of hydroxyl O1 with the increase of its negative charge from −0.810 e to −0.858 e. As a result, this step almost occurred spontaneously, with energy barrier 7.39 kcal/mol as shown in Table 1 and Fig. 2.

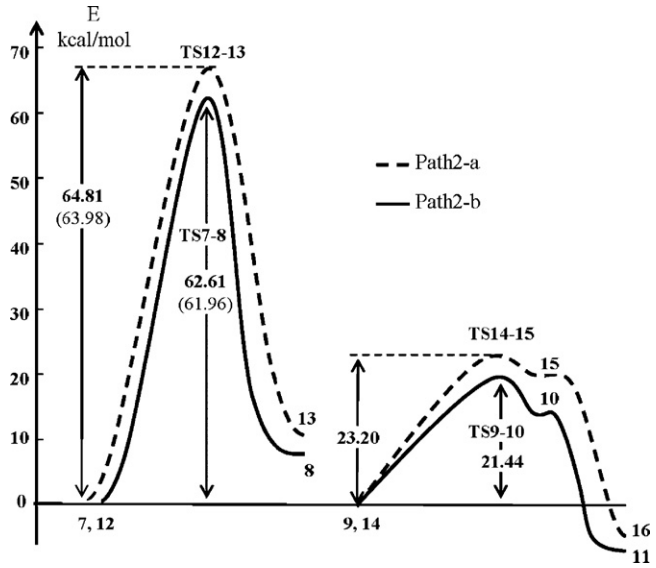

Fig. 3. The total energy (electronic energy + ZPE) curves of CO_2-activated mechanism of synthesis of PC from PG and CO_2 over TBD, calculated at the B3LYP/6-311++G(d,p) level. Energies including BSSE-corrections are also indicated in the parentheses.

It was clear that the charge negativity of O3 and O4 in CO_2 was enhanced gradually from **4** to **5** (see Fig. S1). In contrast, the charge of C4 changed little. The sum of the charges of O3, O4 and C4 was −0.005 e in **4**, while it was −0.156 e in TS4-5 and −0.493 e in **5**. These indicated that from **4** to **5** negative charges were gradually enriched in the region of CO_2, which was one part of the anion $(CH_3)CH(OH)CH_2OC(O)O^-$ in the ion-pair structure **5**. Therefore, the structure **5** might be more stable than **4** due to charge delocalization over the two oxygen atoms, O3 and O4, of the COO^- group. Similar facts were reported by Aresta et al., who investigated the catalytic mechanism of synthesizing DMC from methanol and CO_2, with DCC as catalyst [14].

It should be noted that in structure **5**, the distance between H2 and O3 was 1.760 Å and the bond order was 0.07. So this was actually an intermolecular hydrogen bond, which would stabilize the enriched negative charge on O3 atom as well as the structure of the anion $(CH_3)CH(OH)CH_2OC(O)O^-$. Another point was that the enhanced electronegativity on CO_2 would strengthen the nucleophilic nature of the oxygen center of the carbamate anion [44] and facilitate the nucleophilic attack of O3 on PG in the next dehydration step.

The protonation of the N1 atom in TBD weakened its N2–H3 bond as indicated by the variations of bond length and bond order from structure **4** to **5** (see Fig. S1). In **5**, the intermolecular hydrogen bond H3–O2 between $TBDH^+$ and the other moiety made the deprotonation of N2 favorable. With H3 transferring to O2, **6** was formed, and a nice proton pathway was completed. Thus far, the catalytic role of TBD has been made clear: it functioned as a proton bridge linking the two hydroxyls, and the proton transfer process was powered by the synergistic action of its N atoms.

The unique imaginary frequency of TS5-6 (272.0*i* cm^{-1}) corresponded to the simultaneous stretching vibrations of the O2–C2 bond breaking and the O3–C2 bond forming. Due to the loss of hydroxyl, the NPA charge of the C2 atom increased from 0.106 e (in **5**) to 0.257 e (in TS5-6). The water molecule had already formed in TS5-6 with its charge almost neutral (0.062 e). These indicated that, with the shift of H3 from N2 to the hydroxyl O2 atom of PG, the O2–C2 bond was weakened, which favored the attack of the already nucleophilicly strengthened O3 (mentioned above) on the C2 atom. As a result, the final structure **6** was achieved with the regeneration of TBD. The calculated barrier for the nucleophilic attack of O3 atom on the C2, was 56.96 kcal/mol, which was much higher than the preceding step (7.39 kcal/mol) (see Table 1 and Fig. 2). Thus, this nucleophilic attack was the rate-limiting step of Path1-b.

The reaction process of Path1-a was similar to that of Path1-b, the only difference was that it was the secondary hydroxyl on which the electrophilic attack of CO_2 took place and then the primary hydroxyl was dehydrated. In TS2-3 of Path1-a, the charge of C1 was 0.035 e, which was much lower than that of the C2 in the corresponding transition state TS5-6 of Path1-b. This could lead to the nucleophilic attack of O3 on C1 in Path1-a more difficult than the corresponding nucleophilic attack of O3 on C2 in Path1-b. Consequently, the energy barrier for Path1-a was 63.87 kcal/mol, 6.91 kcal/mol higher than that of Path1-b, indicating the dehydration of secondary hydroxyl was superior to that of primary hydroxyl.

4.2. CO_2-activated mechanism

As in the PG-activated mechanism, there were also two alternative channels, corresponding to dehydration of the primary hydroxyl group (Path2-a) and the secondary one (Path2-b). Here, Path2-b was discussed in detail.

In the initial structure **7** shown in Fig. S2, no intermolecular hydrogen bond was found between the hydroxyl group of PG and the H3 atom of TBD. This was probably due to the steric effect

of TBD–CO_2. This was less favorable for the transfer of H3 to the hydroxyl group than that in the PG-activated mechanism. The unique imaginary frequency of TS7-8 was 238.1*i* cm^{-1}, corresponding to the simultaneous stretching vibrations of the O2 relative to C2 and the O3 atom of TBD–CO_2 relative to C2. Consequently, the old hydroxyl C2–O2 bond broke and the new C2–O3 bond formed with bond length 1.468 Å (bond order 0.82) in structure **8**.

In line with the PG-activated mechanism, the dehydration of the secondary hydroxyl was preferred to the primary hydroxyl, because the NPA charge of C1 (0.092 e in TS12-13) was lower than that of C2 (0.269 e in TS7-8). This indicated that the electrophilic nature of C1 was weaker than C2, which was in agreement with the energy difference (64.81 kcal/mol for TS12-13 and 62.61 kcal/mol for TS7-8, see Table 1 and Fig. 3).

With water molecule leaving away, the intermediate **9** was obtained with the formation of a hydrogen bond between N2 and hydroxyl H1 (bond length 1.902 Å). This was favorable for the proton transfer, which was expected to occur at this position. The imaginary frequency of the succeeding transition state TS9-10 was 275.9*i* cm^{-1}, corresponding to the simultaneous stretching vibrations of O1–C4 and O1–H1. These indicated the proton transfer from the hydroxyl to N2 and the electrophilic attack of C4 atom of CO_2 on O1. Through TS9-10, the PC was formed with the carbonyl C bonded with TBD. The energy cost to pass this step was computed to be 21.44 kcal/mol, which was significantly lower than its preceding step as shown in Fig. 3 and Table 1. In a homogeneous system, structure **10** could transform to structure **11** readily. Thus, the rate-determining step for the CO_2-activated mechanism could be identified as the nucleophilic attack of O atom in CO_2 on to the C atom in PG. The energy barrier was 64.81 kcal/mol for Path2-a and 62.61 kcal/mol for Path2-b.

4.3. Comparison of PG-activated with CO_2-activated mechanism

The theoretical results show that the rate-determining steps corresponded to the particular process of the nucleophilic attack of one of the O atoms in CO_2 on the hydroxyl linked C atom in PG for both the PG-activated and the CO_2-activated mechanisms. The energy analysis suggested that PG-activated mechanism, in which the nucleophile was activated, was favorable than CO_2-activated mechanism. This result agreed with that of Simn and Goodman [32], in which TBD actually activated the nucleophile, methanol, but not the electrophile, lactones in the reaction of TBD-catalyzed ring opening polymerization (ROP) of lactones. As for the two alternative reaction sites of PG, on losing hydroxyl, the C2 atom showed a higher positive charge than the C1 atom and thus a stronger electrophilic ability. So the reaction path with secondary hydroxyl dehydration in PG-activated mechanism has the lowest energy barrier 56.96 kcal/mol. Thus, this path was superior to other reaction paths.

It should be noted that all the energies were not thermally corrected. However, the experimental results show that TBD, as recyclable CO_2 adsorption materials, could fix CO_2 reversibly and release it at higher temperatures [34]. At the optimal conditions of the reaction of PG and CO_2 with TBD as catalyst, the temperature was so high for the stable TBD–CO_2 to exist [4]. Thus, the theoretical results and the real reaction temperature were both not favorable for the CO_2-activated mechanism.

Another point should also be noted. Previous work showed that if placed in acetonitrile, which is a highly polar aprotic solvent, the formation of $TBDH^+$ ion-pair was easier [27]. Furthermore, compared with gas phase the energy barriers of reactions in polar solvents were decreased, which was confirmed by the polarized continuum model (PCM) for the reaction of aliphatic alcohols with CO_2 catalyzed by DCC [14]. Thus, if the solvent effects were to be considered, the energy barriers would be expected to drop.

5. Conclusions

The carbonylation of PG with CO_2 using TBD as catalyst was investigated theoretically by employing DFT method at the B3LYP/6-311++G(d,p) level. The BSSE-corrections were found insignificant at the 6-311++G(d,p) level. Among different proposed mechanisms, the PG-activated route was identified as the most probable reaction path. The rate-determining step was the nucleophilic attack of O atom in CO_2 on the C2 atom in PG with energy barrier 56.96 kcal/mol. The role of TBD was its capability to act as a proton bridge with the synergistic action of its N atoms.

Acknowledgement

This work is financially supported by Chemistry Department, King Saud University.

Appendix A. Supplementary data

Supplementary data associated with this article can be found, in the online version, at doi:10.1016/j.molcata.2009.09.003.

References

[1] Y. Du, D.L. Kong, H.Y. Wang, F. Cai, J.S. Tian, J.Q. Wang, L.N. He, J. Mol. Catal. A 241 (2005) 233–237.
[2] S.Y. Huang, S.G. Liu, J.P. Li, N. Zhao, W. Wei, Y.H. Sun, Catal. Lett. 112 (2006) 187–191.
[3] S.Y. Huang, S.G. Liu, J.P. Li, N. Zhao, W. Wei, Y.H. Sun, J. Fuel Chem. Technol. 35 (2007) 701–705.
[4] S.Y. Huang, J. Ma, J.P. Li, N. Zhao, W. Wei, Y.H. Sun, Catal. Commun. 9 (2008) 276–280.
[5] X.Q. Zhao, N. Sun, S.F. Wang, F. Li, Y.J. Wang, Ind. Eng. Chem. Res. 47 (2008) 1365–1369.
[6] K. Tomishige, H. Yasuda, Y. Yoshida, M. Nurunnabi, B. Li, K. Kunimori, Catal. Lett. 95 (2004) 45–49.
[7] K. Tomishige, H. Yasuda, Y. Yoshida, M. Nurunnabi, B. Li, K. Kunimori, Green Chem. 6 (2004) 206–221.
[8] S.Y. Huang, S.G. Liu, J.P. Li, N. Zhao, W. Wei, Y.H. Sun, Catal. Lett. 118 (2007) 290–294.
[9] W. McGhee, D. Riley, K. Christ, Y. Pan, B. Parnas, J. Org. Chem. 60 (1995) 2820–2830.
[10] M. Abla, J.C. Choi, T. Sakakura, Chem. Commun. (2001) 2238–2239.
[11] T. Yamada, P.J. Lukac, M. George, R.G. Weiss, Chem. Mater. 19 (5) (2007) 967–969.
[12] T. Mizuno, N. Okamoto, T. Ito, T. Miyata, Tetrahedron Lett. 41 (2000) 1051–1053.
[13] E. Haruki, M. Arakawa, N. Matsumura, Y. Otsuji, E. Imoto, Chem. Lett. 3 (1974) 427–428.
[14] M. Aresta, A. Dibenedetto, E. Fracchiolla, P. Giannoccaro, C. Pastore, I. Pápai, G. Schubert, J. Org. Chem. 70 (2005) 6177–6186.
[15] M. Aresta, A. Dibenedetto, C. Pastore, I. Pápai, G. Schubert, Top. Catal. 40 (2006) 71–81.
[16] E.R. Pérez, M.O. da Silva, V.C. Costa, U.P.R. Filho, D.W. Franco, Tetrahedron Lett. 43 (2002) 4091–4093.
[17] R.L. Paddock, Y. Hiyama, J.M. McKay, S.T. Nguyen, Tetrahedron Lett. 45 (2004) 2023–2026.
[18] X.H. Zhang, N. Zhao, W. Wei, Y.H. Sun, Catal. Today 115 (2006) 102–106.
[19] E.R. Pérez, R.H.A. Santos, M.T.P. Gambardella, L.G.M. de Macedo, U.P.R. Filho, J.C. Launay, D.W. Franco, J. Org. Chem. 69 (2004) 8005–8011.
[20] J. Ma, X.L. Zhang, N. Zhao, F.K. Xiao, W. Wei, Y.H. Shun, J. Mol. Struct. (THEOCHEM) 911 (2009) 40–45.
[21] A. Jarczewski, C.D. Hubbard, J. Mol. Struct. 649 (2003) 287–307.
[22] G. Schroeder, B. Łęska, A. Jarczewski, B.N. Wydra, B. Brzezinski, J. Mol. Struct. 344 (1995) 77–88.
[23] G. Schroeder, B. Brzezinski, A. Jarczewski, E. Grech, P. Milart, J. Mol. Struct. 384 (1996) 127–133.
[24] I. Binkowska, J. Koput, A. Jarczewski, J. Mol. Struct. 876 (2008) 344–347.
[25] P. Przybylski, G. Wojciechowski, B. Brzezinski, G. Zundel, F. Bartl, J. Mol. Struct. 661–662 (2003) 171–182.
[26] S.W. Ng, P. Naumov, S. Chantrapromma, S.S.S. Raj, H.-K. Fun, A.R. Ibrahim, G. Wojciechowski, B. Brzezinski, J. Mol. Struct. 569 (2001) 139–145.
[27] A. Jarczewski, J. Koput, I. Nowak, J. Mol. Struct. 788 (2006) 138–144.
[28] B. Brzezinski, G. Schroeder, V.I. Rybachenko, L.I. Kozhevina, V.V. Kovalenko, J. Mol. Struct. 516 (2000) 123–130.
[29] G. Wojciechowskia, G. Schroedera, V. Rybachenkob, B. Brzezinski, J. Mol. Struct. 610 (2002) 81–84.
[30] A. Huczyński, T. Pospieszny, M.R. Sitarz, A. Katrusiak, B. Brzezinski, J. Mol. Struct. 876 (2008) 501–508.

[31] A. Huczyński, I. Binkowska, A. Jarczewski, B. Brzezinski, J. Mol. Struct. 841 (2007) 133–136.
[32] L. Simn, J.M. Goodman, J. Org. Chem. 72 (2007) 9656–9662.
[33] D.J. Heldebrant, P.G. Jessop, C.A. Thomas, C.A. Eckert, C.L. Liotta, J. Org. Chem. 70 (2005) 5335–5338.
[34] F.S. Pereira, E.R. deAzevedo, E.F. da Silva, T.J. Bonagamba, D.L. da Silva Agostíni, A. Magalhães, A.E. Job, E.R. Pérez González, Tetrahedron 64 (2008) 10097–10106.
[35] T. Endo, D. Nagai, T. Monma, H. Yamaguchi, B. Ochiai, Macromolecules 37 (2004) 2007–2009.
[36] M.J. Frisch, G.W. Trucks, H.B. Schlegel, G.E. Scuseria, M.A. Robb, J.R. Cheeseman, J.A. Montgomery Jr., T. Vreven, K.N. Kudin, J.C. Burant, J.M. Millam, S.S. Iyengar, J. Tomasi, V. Barone, B. Mennucci, M. Cossi, G. Scalmani, N. Rega, G.A. Petersson, H. Nakatsuji, M. Hada, M. Ehara, K. Toyota, R. Fukuda, J. Hasegawa, M. Ishida, T. Nakajima, Y. Honda, O. Kitao, H. Nakai, M. Klene, X. Li, J.E. Knox, H.P. Hratchian, J.B. Cross, V. Bakken, C. Adamo, J. Jaramillo, R. Gomperts, R.E. Stratmann, O. Yazyev, A.J. Austin, R. Cammi, C. Pomelli, J.W. Ochterski, P.Y. Ayala, K. Morokuma, G.A. Voth, P. Salvador, J.J. Dannenberg, V.G. Zakrzewski, S. Dapprich, A.D. Daniels, M.C. Strain, O. Farkas, D.K. Malick, A.D. Rabuck, K. Raghavachari, J.B. Foresman, J.V. Ortiz, Q. Cui, A.G. Baboul, S. Clifford, J. Cioslowski, B.B. Stefanov, G. Liu, A. Liashenko, P. Piskorz, I. Komaromi, R.L. Martin, D.J. Fox, T. Keith, M.A. Al-Laham, C.Y. Peng, A. Nanayakkara, M. Challacombe, P.M.W. Gill, B. Johnson, W. Chen, M.W. Wong, C. Gonzalez, J.A. Pople, Gaussian 03, Revision D. 01, Gaussian, Inc., Wallingford, CT, 2004.
[37] A.D. Becke, J. Chem. Phys. 98 (1993) 5648–5652.
[38] R. Krishnan, J.S. Binkley, R. Seeger, J.A. Pople, J. Chem. Phys. 72 (1980) 650–654.
[39] T. Clark, J. Chandrasekhar, G.W. Spitznagel, P.V.R. Schleyer, J. Comput. Chem. 4 (1983) 294–301.
[40] P.M.W. Gill, B.G. Johnson, J.A. Pople, M.J. Frisch, Chem. Phys. Lett. 197 (1992) 499–505.
[41] J.B. Foresman, Æ. Frisch, Exploring Chemistry with Electronic Structure Methods, 2nd ed., Gaussian, Inc, Pittsburgh, PA, 1996.
[42] S.F. Boys, F. Bernardi, Mol. Phys. 19 (1970) 553–566.
[43] S. Simon, M. Duran, J.J. Dannenberg, J. Chem. Phys. 105 (1996) 11024–11031.
[44] W. McGhee, D. Riley, J. Org. Chem. 60 (1995) 6205–6207.